Finite-Horizon Robustness Analysis under Mixed Disturbances using Signal-IQCs

Frederik Thiele * **Harald Pfifer** * **Felix Biertümpfel** *

* *Chair of Flight Mechanics and Control, Technische Universität Dresden, 01069 Dresden, Germany (e-mail: {frederik.thiele, harald.pfifer, felix.biertuempfel}@tu-dresden.de)*

Abstract: Common worst-case analyses for uncertain finite-horizon systems consider quadratic performance metrics based on the strict Bounded Real Lemma. Thus, they assess system performance for bounded inputs, e.g., signals in L2, which exhibit a worst-case shape. Consequently, known disturbance characteristics are left unexploited and uncovered, leading to unnecessarily conservative results. The present paper develops a worst-case analysis covering arbitrarily L2-bounded worst-case signals and partially known disturbances simultaneously. This is achieved by modeling the latter using signal integral-quadratic constraints (IQCs). The resulting analysis condition relies on a dissipation inequality within the IQC framework for finite time horizon problems. This framework also readily allows to incorporate additional system uncertainties in the analysis. The approach's feasibility is demonstrated with the worst-case performance analysis of a small unmanned aerial vehicle in an urban environment.

Keywords: Robust Stability and Performance, Structured and Unstructured Uncertainties, System and Uncertainty Modeling, Integral Quadratic Constraints

1. INTRODUCTION

The induced L_2-norm is a well-established metric for evaluating the performance of key control objectives such as tracking, under the assumption of arbitrary norm-bounded inputs in L_2 over an infinite time horizon. In practice, however, engineering problems often involve external disturbances that are not in L_2, but instead follow specific temporal patterns with known structure. These characteristics arise from the physical properties and environmental conditions of the application. Standard robustness analysis formulations cannot take advantage of prior knowledge and only provide results for the full set of possible disturbances. Furthermore, analyzing a finite time horizon is usually sufficient as performance requirements are often defined over specific time intervals. Typical aerospace applications include space launchers with focus on structural loads during ascent (Biertümpfel et al. (2023b)); missile engagements where the final deviation from the target is critical (Buch (2021)); the response of flexible aircraft to wind gusts (Iannelli et al. (2019)); or auto-land scenarios of aircraft (Biertümpfel and Pfifer (2022)).

This paper proposes a novel formulation for robustness analysis of finite-horizon uncertain systems in the presence of mixed disturbances, i.e., simultaneously considering arbitrary L_2-bounded inputs and signals with partially known characteristics. Such signals could be, e.g., constant biases, bounded arbitrary time-varying behavior or harmonic excitation as considered in Cheah et al. (2024). In the presented work, the known external disturbances are expressed as internal parameter variations driven by an artificial state. This state has an unknown initial value and follows from a non-standard system augmentation. The variation is then bounded using appropriate signal integral quadratic constraints (IQCs), which are particularly suited to recover various signal characteristics. Posing the problem inside the IQC framework also facilitates the incorporation of model uncertainties and nonlinearities in the same analysis. The underlying theorem is derived for the analysis of linear time-varying (LTV) systems with uncertain initial conditions over a finite time horizon.

Applying IQCs to stability and robustness analyses is an established approach introduced by Megretski and Rantzer (1997). Their work derives a frequency-domain stability theorem for uncertain linear time-invariant (LTI) systems based on linear matrix inequalities. Alternatively, time-domain formulations of IQCs, see, e.g., Jönsson (1996), essentially overcome the limitations of LTI systems. They have been applied to the robustness analysis of parameter-varying systems, e.g., in Pfifer and Seiler (2016), time-periodic systems in Ossmann and Pfifer (2019) as well as time-varying systems. The analysis of (uncertain) time-varying systems was conducted in various literature, e.g., in Cantoni et al. (2013) IQCs and a gap metric provide a stability statement; Seiler et al. (2019) discusses bounds of the reachable set and robust induced gains for uncertain finite-horizon systems; and Farhood (2024) addresses uncertain initial conditions. In Biertümpfel et al. (2023a) the robustness of nonlinear systems along uncertain trajectories is analyzed, using a similar system augmentation step as in the presented paper.

⋆ This research was funded by the German Federal Ministry for Economic Affairs and Climate Action under grant number 20Y2109E and partially supported by the European Union under Grant No. 101153910. The responsibility for the content of this paper is with its authors.

The IQC framework has also been applied to cover the effects of specific shapes of external signals, often referred to as signal IQCs. In the works of Jönsson et al. (2003) or Ayala-Cuevas et al. (2019) the impact of oscillations on the system performance is discussed. An evaluation of a flight controller for restricted disturbances is conducted in Palframan et al. (2019) using linear fractional transformation. In Fry et al. (2021) signal IQCs are applied to cover noise in a performance setting, but their approach remains limited to the induced input-output behavior. This shortcoming is addressed with the approach presented in this work.

This paper introduces a novel unified framework that accommodates arbitrary norm-bounded and partially known input signals to provide more realistic analysis results in Section 3. It is applied to the path following problem of an unmanned aerial vehicle (UAV) described in Berenguer Bertran et al. (2025) to evaluate the tracking performance in Section 4. The UAV is subject to model uncertainties and affected by external wind disturbances with known characteristics, while tracking a norm bounded reference command. The results are compared with a classical IQC finite horizon robustness analysis to demonstrate the validity of the proposed approach.

2. UNCERTAIN SYSTEMS OVER FINITE HORIZONS

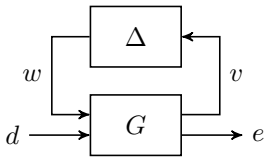

Fig. 1. Interconnection of a nominal LTV system G and perturbation Δ.

An uncertain, finite-horizon linear and possibly time-varying system $\mathcal{F}_u(G,\Delta)$ is defined by the feedback interconnection of a nominal system G and the perturbation Δ as pictured in Fig. 1. The nominal linear system G is:

$$\begin{bmatrix} \dot{x} \\ \hline v \\ e \end{bmatrix} = \left[\begin{array}{c|cc} A & B_w & B_d \\ \hline C_v & D_{vw} & D_{vd} \\ C_e & D_{ew} & D_{ed} \end{array}\right] \begin{bmatrix} x \\ \hline w \\ d \end{bmatrix}, \tag{1}$$

where $x(t) \in \mathbb{R}^{n_x}$, $d(t) \in \mathbb{R}^{n_d}$, and $e(t) \in \mathbb{R}^{n_e}$ denote the state, disturbance input, and performance output vector at time t, respectively. The connection between the system G and perturbation Δ is provided by the vectors $w(t) \in \mathbb{R}^{n_w}$ and $v(t) \in \mathbb{R}^{n_v}$, i.e. $w = \Delta(v)$. The matrices A, B, C, and D are piecewise continuous locally bounded matrix-valued functions of time with dimensions corresponding to the multiplied vectors. The explicit time dependence is mostly omitted in this paper for brevity and will be clear from context. The uncertainty $\Delta : L_2^{n_v}[0,T] \to L_2^{n_w}[0,T]$ is a bounded and causal operator. It can describe nonlinearities like saturation, infinite-dimensional operators such as time delays, as well as dynamic and real parametric uncertainties.

In this paper, the input-output behavior of the perturbation Δ is bounded with time-domain IQCs. A time-domain IQC is defined by a stable filter $\Psi \in \mathbb{RH}_\infty^{n_z \times (n_v+n_w)}$ with the output $z \in \mathbb{R}^{n_z}$ and a real symmetric matrix $M = M^T \in \mathbb{R}^{n_z \times n_z}$ as described in Pfifer and Seiler (2016). If the output z of the filter Ψ satisfies the quadratic time-constraint

$$\int_0^T z(t)^T M z(t)\, dt \geq 0 \tag{2}$$

for all $v \in L_2[0,T]$ and $w = \Delta(v)$ over the interval $[0,T]$, the uncertainty Δ satisfies the IQC defined by M and Ψ. This will be indicated by the short notation $\Delta \in IQC(\Psi, M)$.

From the worst-case analysis of nominal LTV systems in Green and Limebeer (1994) and the finite-horizon time-domain IQC formulation of the perturbation Δ, a worst-case gain condition can be derived as shown in Biertümpfel and Pfifer (2018) and Seiler et al. (2019). It provides a guaranteed upper bound on the input-output behavior of an uncertain LTV system over the considered finite analysis horizon. Given a perturbation satisfying an IQC represented by (Ψ, M), i.e. $\Delta \in IQC(\Psi, M)$, the interconnection $\mathcal{F}_u(G,\Delta)$ can be extended by the IQC filter Ψ. This procedure is illustrated in Fig. 2. The

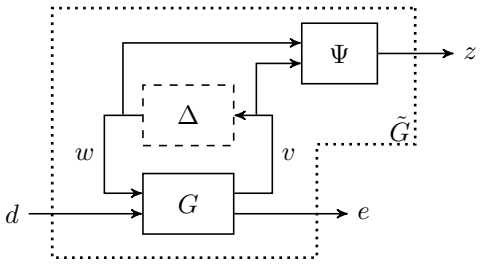

Fig. 2. Extended state-space system $\tilde{G}$.

dynamics of this interconnection is referred to as $\tilde{G}$ and defined by

$$\begin{bmatrix} \dot{\tilde{x}} \\ \hline z \\ e \end{bmatrix} = \left[\begin{array}{c|cc} \tilde{A} & B_1 & B_2 \\ \hline C_1 & D_{11} & D_{12} \\ C_2 & D_{21} & D_{22} \end{array}\right] \begin{bmatrix} \tilde{x} \\ \hline w \\ d \end{bmatrix}. \tag{3}$$

In (3), $\tilde{x}(t)$ contains the states of G and Ψ. By enforcing the time-domain inequality (2) on the filter output z, the explicit representation of the uncertainty $w = \Delta(v)$ is replaced. The finite horizon worst-case induced $L_2[0,T]$-gain is defined as

$$\|\mathcal{F}_u(G,\Delta)\|_{2[0,T]} := \sup_{\Delta \in \mathrm{IQC}(\Psi,M)} \sup_{\substack{d \in L_2[0,T] \\ d \neq 0, x(0)=0}} \frac{\|e\|_{2[0,T]}}{\|d\|_{2[0,T]}}, \tag{4}$$

with, e.g., $\|d\|_{2[0,T]} = [\int_0^T d(t)^T d(t) \mathrm{d}t]^{\frac{1}{2}}$. This gain can be interpreted as a bound on the energy amplification from the disturbance input to the performance output over the time horizon $[0,T]$ and all $\Delta \in IQC(\Psi, M)$. A dissipation inequality can be stated to upper bound the worst-case induced $L_2[0,T]$-gain of the interconnection $\mathcal{F}_u(G,\Delta)$. It is based on the extended LTV system $\tilde{G}$ given by (3) and the finite horizon time-domain IQC formulation in (2). This dissipation inequality is rearranged as an equivalent Riccati differential equation (RDE) formulation in the following Theorem 1:

Theorem 1. Let $\mathcal{F}_u(G,\Delta)$ be well-posed $\forall\, \Delta \in IQC(\Psi, M)$, then $\|F_u(G,\Delta)\|_{2[0,T]} < \gamma$ if there exist a continuously differentiable symmetric $P : \mathbb{R}_0^+ \to \mathbb{R}^{n_x \times n_x}$ such that

$$P(T) = 0, \tag{5}$$

$$\dot{P} = \hat{Q} + P\hat{A} + \hat{A}^T P - P\hat{S}P \qquad \forall t \in [0,T] \tag{6}$$

and

$$\hat{R} = \begin{bmatrix} D_{11}^T M D_{11} + D_{21}^T D_{21} & D_{11}^T M D_{12} + D_{21}^T D_{22} \\ D_{12}^T M D_{11} + D_{22}^T D_{21} & D_{12}^T M D_{12} + D_{22}^T D_{22} - \gamma^2 I_{n_d} \end{bmatrix} < 0, \tag{7}$$

with

$$\hat{A} = \begin{bmatrix} B_1 & B_2 \end{bmatrix} \hat{R}^{-1} \begin{bmatrix} (C_1^T M D_{11} + C_2^T D_{21})^T \\ (C_1^T M D_{12} + C_2^T D_{22})^T \end{bmatrix} - \tilde{A}, \tag{8}$$

$$\hat{S} = -\begin{bmatrix} B_1 & B_2 \end{bmatrix} \hat{R}^{-1} \begin{bmatrix} B_1^T \\ B_2^T \end{bmatrix}, \tag{9}$$

and

$$\begin{aligned} \hat{Q} = &- C_1^T M C_1 - C_2^T C_2 \\ &+ \begin{bmatrix} (C_1^T M D_{11} + C_2^T D_{21})^T \\ (C_1^T M D_{12} + C_2^T D_{22})^T \end{bmatrix}^T \hat{R}^{-1} \begin{bmatrix} (C_1^T M D_{11} + C_2^T D_{21})^T \\ (C_1^T M D_{12} + C_2^T D_{22})^T \end{bmatrix}. \end{aligned} \tag{10}$$

Proof. The proof is provided in Biertümpfel and Pfifer (2018).

For a more thorough description, the reader is referred to the work of Seiler et al. (2019) and Biertümpfel et al. (2023b). Therein, efficient approaches for computing an upper bound on the worst-case gain are provided.

Remark: Theorem 1 is limited to the analysis of arbitrary $L_2[0,T]$ worst-case disturbances maximizing the induced $L_2[0,T]$-gain. Corollaries of this theorem can cover other quadratic performance metrics but are limited to induced input-output gains. It is also possible to include different performance metrics in one analysis using dedicated performance blocks, see, e.g., Fry et al. (2021). However, these blocks are limited to specific input-output pairs, i.e., there is a one-to-one correspondence between a specific disturbance and performance output. Hence, mixed disturbance signals affecting one or more performance outputs cannot be covered. For example, assume that Theorem 1 is applied to a problem with two disturbances affecting a single output. One is well represented by an arbitrarily shaped norm-bounded signal. The other has a known maximum amplitude but otherwise arbitrary shape. However, the analysis will simply provide an upper bound for the worst-case combination of both signals. The maximum amplitude of the second disturbance cannot be enforced, which yields inaccurate results.

3. ANALYSIS OF MIXED-DISTURBANCES USING SIGNAL IQCS

3.1 Analysis Condition

This section derives a novel formulation for robustness analysis that allows to account for mixed disturbances. In particular, the analysis considers arbitrary norm-bounded worst-case signals and signals with (partially) a priori known properties affecting the same performance output. The latter will be incorporated using *signal IQCs* effectively decoupling them from the former. Consider a finite-horizon linear system with the external disturbances d and δ

$$\left[\begin{array}{c} \dot{x} \\ \hline e \end{array}\right] = \left[\begin{array}{c|cc} A & B_d & B_\delta \\ \hline C & D_d & D_\delta \end{array}\right] \begin{bmatrix} x \\ d \\ \delta \end{bmatrix}, \tag{11}$$

where $d \in L_2^{n_d}[0,T]$ are norm-bounded arbitrary disturbance signals and $\delta(t) \in \mathbb{R}^{n_\delta}$ are disturbances with partially known characteristics. The disturbance signals δ are multiplied by a constant driving term with value 1. Extending the state vector with this driving term pushes the term $B_\delta \delta$ into the state matrix and $D_\delta \delta$ into the output matrix. The resulting state-space representation is:

$$\left[\begin{array}{c} \dot{x} \\ 0 \\ \hline e \end{array}\right] = \left[\begin{array}{cc|c} A & B_\delta \delta & B_d \\ 0 & 0 & 0 \\ \hline C & D_\delta \delta & D_d \end{array}\right] \left[\begin{array}{c} x \\ 1 \\ \hline d \end{array}\right]. \tag{12}$$

This system is non-standard but identical to the system (11). In the next step, the driving term is replaced with an artificial state $x_\delta := 1$ providing the augmented system:

$$\left[\begin{array}{c} \dot{x} \\ 0 \\ \hline e \end{array}\right] = \left[\begin{array}{cc|c} A & B_\delta \delta & B_d \\ 0 & 0 & 0 \\ \hline C & D_\delta & D_d \end{array}\right] \left[\begin{array}{c} x \\ x_\delta \\ \hline d \end{array}\right]. \tag{13}$$

As the signals δ have known properties, they can without loss of generality be confined to a set of expected disturbances $\mathcal{D} \subseteq \mathbb{R}^{n_\delta}$. By restricting the disturbance signals δ to this set, they can be treated equivalently as perturbations $\Delta_\mathrm{S} := \mathrm{diag}(\delta_1, \delta_2, \ldots, \delta_{n_\delta})$. The external disturbances thus become internal signals described by Δ_S which are driven by a single artificial state. In other words, one artificial state is sufficient to persistently excite multiple internal signals. An uncertain finite-horizon system comparable to (1) can be recovered which provides the system H:

$$\begin{aligned} \left[\begin{array}{c} \dot{x} \\ 0 \\ \hline v_\delta \\ e \end{array}\right] &= \left[\begin{array}{cc|cc} A & 0 & B_\delta & B_d \\ 0 & 0 & 0 & 0 \\ \hline 0 & 1_{n_\delta} & 0 & 0 \\ C & 0 & D_\delta & D_d \end{array}\right] \left[\begin{array}{c} x \\ x_\delta \\ \hline w_\delta \\ d \end{array}\right] \\ w_\delta &= \Delta_\mathrm{S}(v_\delta), \end{aligned} \tag{14}$$

with $v_\delta(t) \in \mathbb{R}^{n_\delta} := x_\delta$, $w_\delta(t) \in \mathbb{R}^{n_\delta}$, and 1_{n_δ} the 1-vector of size n_δ. The input-output behavior of these internal signals can be upper bounded with a suitable signal IQC, such that $\Delta_\mathrm{S} \in IQC(\Psi, M)$. Extending the system (14) with the IQC filter Ψ yields the state-space system required for an IQC-based analysis:

$$\left[\begin{array}{c} \dot{\bar{x}} \\ z \\ \hline e \end{array}\right] = \left[\begin{array}{c|cc} \mathcal{A} & \mathcal{B}_1 & \mathcal{B}_2 \\ \hline \mathcal{C}_1 & \mathcal{D}_{11} & \mathcal{D}_{12} \\ \mathcal{C}_2 & \mathcal{D}_{21} & \mathcal{D}_{22} \end{array}\right] \left[\begin{array}{c} \bar{x} \\ w_\delta \\ \hline d \end{array}\right]. \tag{15}$$

This extended system is closely related to $\tilde{G}$ in (3), but its extended state vector $\bar{x}$ also contains the artificial state $x_\delta := 1$, i.e., $\bar{x} = [\tilde{x}^T, x_\delta]^T$. Theorem 1 provides an analysis condition to bound the worst-case induced $L_2[0,T]$ gain in (4) for zero initial conditions. Thus, it cannot be applied directly to this problem. Extensions of the (nominal) Bounded Real Lemma (BRL) to uncertain initial conditions as in Khargonekar et al. (1991) provide corresponding bounds for induced gains. These have numerators of the form $\sqrt{\|d\|_{2[0,T]}^2 + x^T(0) N x(0)}$. Here, the matrix $N > 0 \in \mathbb{R}^{n_x \times n_x}$ quantifies the *relative importance* of the initial condition with respect to the external disturbances. Thus, $x(0)$ cannot be restricted to a specific set as required in (14).

To derive a suitable analysis condition, we exploit the fact that for zero initial conditions any disturbance can be scaled such that $\|d\|_{2[0,T]} = 1$. In this case, Theorem 1 provides an upper bound on the performance output $\|e\|_{2[0,T]} \leq \gamma$. The following theorem provides an analysis

condition to calculate an upper bound on the worst-case $L_2[0,T]$-norm of the performance output $\|e\|_{2[0,T]}$ which confines the artificial state x_δ to $\{x_\delta \in \mathbb{R} : |x_\delta| \leq 1\}$ and also enforces $\|d\|_{2[0,T]} \leq 1$.

Theorem 2. Let $\mathcal{F}_u(H, \Delta_\mathrm{S})$ be well-posed for all $\Delta_\mathrm{S} \in IQC(\Psi, M)$. Then the worst case $L_2[0,T]$ norm of the performance output e is bounded by the scalar $\gamma > 0$ for $\|d\|_{2[0,T]} \leq 1$ and $|x_\delta(0)| \leq 1$ if there exist scalars $\alpha_1 > 0$ and $\alpha_2 > 0$, and a continuously differentiable symmetric matrix function $P(t) = \begin{bmatrix} P_{11} & P_{12} \\ P_{12}^T & P_{22} \end{bmatrix}$ such that

$$\begin{bmatrix} \dot{P} + P\mathcal{A} + \mathcal{A}^T P & P\mathcal{B}_1 & P\mathcal{B}_2 \\ \mathcal{B}_1^T P & 0 & 0 \\ \mathcal{B}_2^T P & 0 & -I \end{bmatrix} + \begin{bmatrix} \mathcal{C}_1^T \\ \mathcal{D}_{11} \\ \mathcal{D}_{12}^T \end{bmatrix} M \begin{bmatrix} \mathcal{C}_1^T \\ \mathcal{D}_{11}^T \\ \mathcal{D}_{12}^T \end{bmatrix}^T + \alpha_2 \begin{bmatrix} \mathcal{C}_2^T \\ \mathcal{D}_{21} \\ \mathcal{D}_{22}^T \end{bmatrix} \begin{bmatrix} \mathcal{C}_2^T \\ D_{21}^T \\ \mathcal{D}_{22}^T \end{bmatrix}^T < 0 \tag{16}$$

and

$$\begin{bmatrix} P_{22}(0) - \alpha_1 & 0 & 0 \\ 0 & -P(T) & 0 \\ 0 & 0 & \alpha_1 - \alpha_2\gamma^2 + 1 \end{bmatrix} \leq 0 \tag{17}$$

Proof. The proof relies on the definition of a time-varying quadratic storage function $V(\bar{x}, t) = \bar{x}(t)^T P(t)\bar{x}(t)$ and uses a standard dissipation argument. Perturbing the left-hand-side of (16) with $(1-\epsilon)$ with $0 < \epsilon \ll 1$, multiplying the left and right side with $[\bar{x}^T, w_\delta^T, d^T]$ and $[\bar{x}^T, w_\delta^T, d^T]^T$, respectively yields

$$\dot{V}(\bar{x}, t) + z^T M z + \alpha_2 e^T e - (1-\epsilon) d^T d \leq 0. \tag{18}$$

Integrating this dissipation inequality from 0 to T and recalling that only $x_\delta(0) \neq 0$ provides

$$\bar{x}(T)^T P(T)\bar{x}(T) - x_\delta(0)^2 P_{22}(0) + \int_0^T z(t)^T M z(t) dt + \alpha_2 \|e\|_{2[0,T]}^2 - (1-\epsilon)\|d\|_{2[0,T]}^2 \leq 0. \tag{19}$$

Multiplying the left-hand-side of (17) with $[x_\delta(0), \bar{x}(T)^T, 1]$ and $[x_\delta(0), \bar{x}(T)^T, 1]^T$, respectively results in

$$x_\delta(0)^2 P_{22}(0) - \alpha_1 x_\delta(0)^2 - \bar{x}(T)^T P(T)\bar{x}(T) + \alpha_1 - \alpha_2\gamma^2 + 1 \leq 0. \tag{20}$$

As $\Delta_\mathrm{S} \in IQC(\Psi, M)$, it follows that $\int_0^T z(t)^T M z(t) dt \geq 0$ and (19) can be substituted into (20) which yields the inequality

$$1 - (1-\epsilon)\|d\|_{2[0,T]}^2 + \alpha_2(\|e\|_{2[0,T]}^2 - \gamma^2) + \alpha_1(1 - x_\delta(0)^2) \leq 0. \tag{21}$$

From the definitions $\|d\|_{2[0,T]} \leq 1$ and $|x_\delta| \leq 1$, it can be concluded that $\|e\|_{2[0,T]} \leq \gamma$. □

Note that in the analysis only the artificial state x_δ has non-zero initial conditions. Accordingly, Theorem 2 partitions P into a $n_{\bar{x}} \times n_{\bar{x}}$ matrix P_{11} (related to the state $\tilde{x}$) and a scalar P_{22} (related to the artificial state x_δ). The upper left entry in (17) constrains the initial value $x_\delta(0)$.

3.2 Computational approach

A few steps are necessary to convert Theorem 2 into a computationally tractable problem. First, an infinite number of feasible IQCs exists to bound the behavior of a given signal. The most common solution to this problem found in literature, e.g., Veenman et al. (2016) or Pfifer and Seiler (2016), uses a fixed IQC filter Ψ and parameterizes M. In other words, M is restricted to a feasible set $\mathcal{M}$ such that $\Delta_\mathrm{S} \in IQC(\Psi, M)$. In Megretski and Rantzer (1997) and Veenman et al. (2016) extensive catalogs of IQCs suitable to describe different types of signals are provided. Two examples for useful IQC parameterizations for signals are given below. The first example concerns a constant disturbance whose absolute value is known to be bounded.

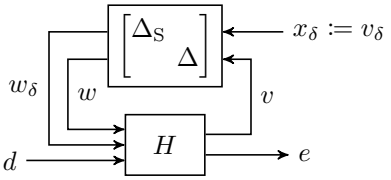

Fig. 3. Analysis setup concept with system uncertainties

Example 3. (Constant Disturbance). Let $\Delta_\mathrm{S} = \delta$ be a constant signal δ, with $|\delta(t)| \leq b \in \mathbb{R}$. A valid time-domain IQC for Δ_S is defined by $\Psi = \mathrm{diag}(\psi_\nu, \psi_\nu)$ and $\mathcal{M} := \{M = \begin{bmatrix} b^2 X & Y \\ Y^T & -X \end{bmatrix} : X = X^T > 0 \in \mathbb{R}^{(\nu+1)\times(\nu+1)}, Y = -Y^T \in \mathbb{R}^{(\nu+1)\times(\nu+1)}\}$. A typical choice for $\psi_\nu \in \mathbb{RH}_\infty^{(\nu+1)\times 1}$ is $\psi_\nu = \begin{bmatrix} 1 & \frac{s+\rho}{s-\rho} & \dots & \frac{(s+\rho)^\nu}{(s-\rho)^\nu} \end{bmatrix}^T$, $\rho < 0$, $\nu \in \mathbb{N}_0$.

This example may appear trivial, but constant external disturbances, e.g., biases, cannot be covered in standard BRL-based worst-case analyses. The next example describes an arbitrarily time-varying unknown disturbance signal with bounded maximum amplitude.

Example 4. (Time-Varying Disturbance). Let $\Delta_\mathrm{S} = \delta$ be an arbitrarily time-varying signal, with $|\delta(t)| \leq b \in \mathbb{R}\, \forall\, t \in [0,T]$. A valid time-domain IQC for Δ_S is defined by $\Psi = \begin{bmatrix} 1 & 0 \\ 0 & 1 \end{bmatrix}$ and $\mathcal{M} := \{M = \begin{bmatrix} b^2 X & 0 \\ 0 & -X \end{bmatrix} : X > 0 \in \mathbb{R}\}$.

After choosing a suitable IQC parmeterization, the remainder of the theorem is addressed. The LMI (16) has to hold for all $t \in [0,T]$, which poses an infinite number of constraints. The most common approach to render the analysis condition computationally feasible is to enforce the inequality condition only on a finite set of i grid points $t_i \in [0,T]$, see, e.g., Pfifer and Seiler (2016). The decision variables in conditions (16) and (17) are the matrix function P, the IQC parameterization $M \in \mathcal{M}$, and the positive scalars α_1 and α_2. The time-varying function P must also be constrained to a finite dimensional subspace to pose a computationally tractable problem. Most commonly, these are expressed as linear combinations, e.g. $P(t) = \sum_{i=0}^{N_\mathrm{b}} t^i P_i$, $i = 0, 1, ..., N_\mathrm{b}$, where N_b denotes the order of the basis function. Thus, the coefficients P_i become the decision variables. More sophisticated basis functions like cubic splines can also be employed, as in Seiler et al. (2019). Feasible coefficients can then be calculated using a semidefinite program with the constraints (16) and (17) for a given γ. Bisecting over γ calculates the minimal feasible upper bound on $\|e\|_{2[0,T]}$.

Additional uncertainties Δ in the system dynamics can be readily included by following the explanations in Section 2. Doing so results in an extended uncertainty block $\mathbf{\Delta} := \mathrm{diag}(\Delta_\mathrm{S}, \Delta)$ in Theorem 2. Figure 3 provides an graphical interpretation of the corresponding analysis setup for the system H in (14) including an additional uncertainty $w = \Delta(v)$ analog to (1).

4. NUMERICAL EXAMPLE: UAV PATH-FOLLOWING ANALYSIS

This section presents a robustness analysis of a load factor tracker of an UAV under wind turbulence and system uncertainties. The controller was developed as part of the integrated guidance and robust control architecture for following energy optimal flight paths in urban environments (Berenguer Bertran et al. (2025)). Here, robustness is crucial, as the trajectory is in the proximity of buildings to maximize the energy savings.

4.1 Augmented Aircraft Model

The nonlinear longitudinal dynamics of the UAV are linearized for a velocity of 17 m/s and an altitude of 20 m. The resulting state-space representation is defined by the state vector $x = [U\ W\ \theta\ q]^T$, with the pitch angle θ, pitch rate q and the velocities U and W in the aircraft's body-fixed frame pointing in the direction of the nose and downwards, respectively. The system's inputs are the horizontal wind component δ_w and the elevator deflection δ_e. The expected wind disturbance is based on measurements taken in the city of Dresden, Germany. Specifically, it corresponds to the average of the mean hourly wind speeds during the year's windiest day. The maximum amplitude of the wind disturbance is bounded by $|\delta_w| \leq b_{\delta_w} = 5\,\mathrm{m/s}$. The wind disturbance is included in the robustness analysis following the steps in Section 3 which leads to an augmented state-space system with the artificial state x_{δ_w} acting as a driving term. The augmented system G_UAV is:

$$\begin{bmatrix}\dot{U}\\ \dot{W}\\ \dot{\theta}\\ \dot{q}\\ 0\end{bmatrix} = \begin{bmatrix}-0.19 & 0.32 & -9.8 & 1.02 & 0.14\,\delta_w\\ -1.58 & -6.32 & 0.67 & 15.1 & 0.63\,\delta_w\\ 0 & 0 & 0 & 1 & 0\\ -0.25 & -3.75 & 0 & -12.5 & -0.01\,\delta_w\\ 0 & 0 & 0 & 0 & 0\end{bmatrix}\begin{bmatrix}U\\ W\\ \theta\\ q\\ x_{\delta_w}\end{bmatrix} + \begin{bmatrix}-0.013\\ 0\\ -0.19\\ -0.98\\ 0\end{bmatrix}\delta_e$$

$$n_z = \begin{bmatrix}0.16 & 0.64 & 0 & 0.19 & -0.06\,\delta_w\end{bmatrix}\begin{bmatrix}U\\ W\\ \theta\\ q\\ x_{\delta_w}\end{bmatrix} + 0.0194\,\delta_e, \tag{22}$$

with n_z denoting the load factor. The control objective is to track the reference load factor $n_{z,\mathrm{cmd}}$. The reference value is provided by an outer loop flight path and airspeed controller. The command can be reasonably assumed as an arbitrary norm-bounded signal, i.e., $n_{z,\mathrm{cmd}} \in L_2$; a common assumption to assess tracking performance. It is filtered through a low-pass filter G_F with a roll-off at 7 rad/s to account for the control bandwidth of the outer loop controller. The load factor controller is

$$K_{n_z} = \frac{-726.7s^2 - 1.308\cdot 10^4 s - 5.831\cdot 10^4}{s^3 + 57.4s^2 + 810s}. \tag{23}$$

The elevator actuator is modeled by a first order lag G_Act with a time constant $T_\mathrm{Act} = 0.02$ s. Uncertainties in the system dynamics are modeled as a multiplicative dynamic uncertainty Δ at the actuator input. The uncertainty Δ is a SISO LTI system with $\|\Delta\|_\infty \leq b_\Delta$. For the presented example the uncertainty level is set to 60%, i.e., $b_\Delta = 0.6$. The uncertain closed loop interconnection of the analysis problem is shown in Fig. 4, with the performance output $e = n_{z,\mathrm{cmd}} - n_z$.

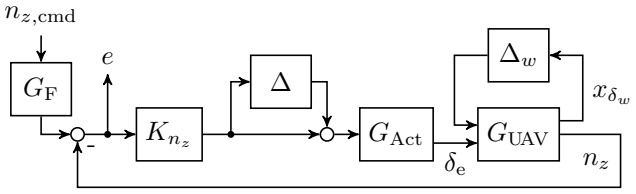

Fig. 4. Analysis setup for load factor tracker.

4.2 Robustness Analysis

The analysis horizon is set to $T = 3$ s. This is motivated by the fact that load factor variations mostly occur during turn maneuvers. In an urban scenario, these are usually completed within a few seconds. To apply the analysis condition in Theorem 2 and calculate the bound on the worst case $\|e\|_{2[0,T]}$, the interconnection in Fig. 4 must be transferred into the IQC framework as detailed in Section 2. The model uncertainty Δ is represented by the an IQC resembling a SISO LTI dynamic uncertainty, see, e.g., Veenman et al. (2016). This means, $\Delta \in IQC(\Psi, M)$ with $M = \left[\begin{smallmatrix} b_\Delta X & 0 \\ 0 & -X\end{smallmatrix}\right]$ and $\Psi = \left[\begin{smallmatrix}\psi_\nu & 0\\ 0 & \psi_\nu\end{smallmatrix}\right]$. The basis function is chosen as $\psi_\nu = \left[\begin{smallmatrix}1 & \frac{1}{s+1}\end{smallmatrix}\right]^T$.
The turbulent wind δ_w is approximated by an arbitrarily fast time-varying disturbance signal which can be modeled with the IQC given in Example 4, i.e. $\Delta_w \in IQC(\Psi_w, M_w)$, with the factorization $\Psi_w = \left[\begin{smallmatrix}1 & 0\\ 0 & 1\end{smallmatrix}\right]$ and parameterization $M_w = \left[\begin{smallmatrix} b_{\delta_w} X & 0 \\ 0 & -X\end{smallmatrix}\right]$. A third-order polynomial basis functions represents P. The conditions of Theorem 2 are evaluated for a finite number of LMIs along an equidistant time grid with a step size of 0.1 s. The resulting semi-definite program is solved using Matlab's `lmilab`. A bisection over γ yields the performance gain $\gamma = 4.98$.

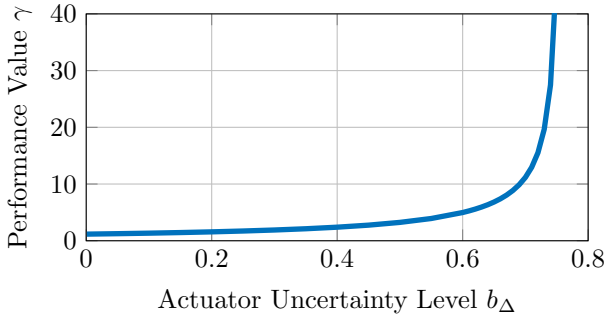

Fig. 5. Robust performance for different actuator uncertainty levels.

The performance analysis was repeated for a total of 30 different uncertainty levels distributed between 0 and 80%, i.e., $b_\Delta \in [0\ 0.8]$. The wind disturbance remains bounded by the previously defined signal IQC Δ_w with $b_{\delta_w} = 5.5$

m/s. The results are depicted in Fig. 5 and show the expected exponential increase in the performance value γ, thus verifying that traditional uncertainty descriptions are captured correctly within the novel approach.

5. CONCLUSION

This paper contributes a novel worst-case performance analysis that incorporates the specific characteristics of partially known disturbances while simultaneously considering worst-case norm-bounded inputs. The partially known disturbances are accounted for through variations of an internal signal of the system which is bounded by an appropriate signal integral quadratic constraints. This approach removes restrictions imposed by frameworks relying on induced norms for the analysis of systems under mixed disturbances, such as one-to-one correspondence between specific performance inputs and outputs. The corresponding analysis condition provides an upper bound on the $L_2[0,T]$ norm of the performance output, which establishes a relationshipt to classical induced norm approaches. The approach is applied to the path-tracking task of an UAV.

REFERENCES

Ayala-Cuevas, J., Saggin, F., Korniienko, A., and Scorletti, G. (2019). Stability analysis of time-varying systems with harmonic oscillations using IQC frequency domain multipliers. In *2019 IEEE 58th Conference on Decision and Control (CDC)*, 5193–5198. doi:10.1109/CDC40024.2019.9029738.

Berenguer Bertran, R., Biertümpfel, F., and Pfifer, H. (2025). Guidance and control of an unmanned aerial vehicle along energy optimal trajectories. In *AIAA SCITECH 2025 Forum*. doi:10.2514/6.2025-0320.

Biertümpfel, F., Theis, J., and Pfifer, H. (2023a). Robustness analysis of nonlinear systems along uncertain trajectories. *IFAC-PapersOnLine*, 56(2), 5831–5836. doi:10.1016/j.ifacol.2023.10.075. 22nd IFAC World Congress.

Biertümpfel, F. and Pfifer, H. (2018). Worst case gain computation of linear time-varying systems over a finite horizon. In *2018 IEEE Conference on Control Technology and Applications (CCTA)*, 952–957. doi:10.1109/CCTA.2018.8511591.

Biertümpfel, F. and Pfifer, H. (2022). Finite horizon analysis of autolanded aircraft in final approach under crosswind. *Control Engineering Practice*, 122, 105105. doi:https://doi.org/10.1016/j.conengprac.2022.105105.

Biertümpfel, F., Pholdee, N., Bennani, S., and Pfifer, H. (2023b). Finite horizon worst case analysis of linear time-varying systems applied to launch vehicle. *IEEE Transactions on Control Systems Technology*, 31(6), 2393–2404. doi:10.1109/TCST.2023.3260728.

Buch, J. (2021). *Finite Horizon Robustness with Applications to Missile Engagements*. Ph.D. thesis, University of Minnesota.

Cantoni, M., Jönsson, U.T., and Khong, S.Z. (2013). Robust stability analysis for feedback interconnections of time-varying linear systems. *SIAM Journal on Control and Optimization*, 51(1), 353–379. doi:10.1137/100814676.

Cheah, S.K., Bhattacharjee, D., Hemati, M., and Caverly, R. (2024). Control synthesis for a hypersonic vehicle with harmonic excitation inputs and input-output-sampled nonlinearities. In *AIAA SCITECH 2024 Forum*. doi:10.2514/6.2024-1589.

Farhood, M. (2024). Robustness analysis of uncertain time-varying systems with unknown initial conditions. *International Journal of Robust and Nonlinear Control*, 34(4), 2472–2495. doi:10.1002/rnc.7094.

Fry, J.M., Abou Jaoude, D., and Farhood, M. (2021). Robustness analysis of uncertain time-varying systems using integral quadratic constraints with time-varying multipliers. *International Journal of Robust and Nonlinear Control*, 31(3), 733–758. doi:10.1002/rnc.5299.

Green, M. and Limebeer, D.J.N. (1994). *Linear robust control*. Prentice-Hall, Inc., USA.

Iannelli, A., Seiler, P., and Marcos, A. (2019). Worst-case disturbances for time-varying systems with application to flexible aircraft. *Journal of Guidance, Control, and Dynamics*, 42(6), 1261–1271. doi:10.2514/1.G004023.

Jönsson, U. (1996). *"Robustness Analysis of Uncertain and Nonlinear Systems*. Ph.D. thesis, Lund Institute of Technology.

Jönsson, U., Kao, C.Y., and Megretski, A. (2003). Analysis of periodically forced uncertain feedback systems. *IEEE Transactions on Circuits and Systems I: Fundamental Theory and Applications*, 50(2), 244–258. doi:10.1109/TCSI.2002.808218.

Khargonekar, P.P., Nagpal, K.M., and Poolla, K.R. (1991). H-infinity control with transients. *SIAM Journal on Control and Optimization*, 29(6), 1373–1393. doi:10.1137/0329070.

Megretski, A. and Rantzer, A. (1997). System analysis via integral quadratic constraints. *IEEE Transactions on Automatic Control*, 42(6), 819–830. doi:10.1109/9.587335.

Ossmann, D. and Pfifer, H. (2019). Robustness analysis of continuous periodic systems using integral quadratic constraints. In *2019 IEEE 58th Conference on Decision and Control (CDC)*, 5805–5810. doi:10.1109/CDC40024.2019.9029808.

Palframan, M.C., Fry, J.M., and Farhood, M. (2019). Robustness analysis of flight controllers for fixed-wing unmanned aircraft systems using integral quadratic constraints. *IEEE Transactions on Control Systems Technology*, 27(1), 86–102. doi:10.1109/TCST.2017.2766598.

Pfifer, H. and Seiler, P. (2016). Less conservative robustness analysis of linear parameter varying systems using integral quadratic constraints. *International Journal of Robust and Nonlinear Control*, 26(16), 3580–3594. doi:10.1002/rnc.3521.

Seiler, P., Moore, R.M., Meissen, C., Arcak, M., and Packard, A. (2019). Finite horizon robustness analysis of LTV systems using integral quadratic constraints. *Automatica*, 100, 135–143. doi:10.1016/j.automatica.2018.11.009.

Veenman, J., Scherer, C.W., and Köroğlu, H. (2016). Robust stability and performance analysis based on integral quadratic constraints. *European Journal of Control*, 31, 1–32. doi:10.1016/j.ejcon.2016.04.004.